Journal of Computational Applied Mechanics 2021, 52(1)
DOI: 10.22059/jcamech.2020.310491.559

RESEARCH PAPER

Evaluating computational performances of hyperelastic models on supraspinatus tendon uniaxial tensile test data

H.M. Ngwangwa[1,*], F. Nemavhola[1]

[1]Biomechanics Research Group, Department of Mechanical and Industrial Engineering, School of Engineering, College of Science, Engineering and Technology, University of South Africa, Private Bag X6, Florida, 1710, Johannesburg, South Africa.

Abstract

Accurate modelling of the mechanical behaviour of tendon tissues is vital due to their essential role in the facilitation of joint mobility in humans and animals. This study focuses on the modelling of the supraspinatus tendon which helps to maintain dynamic stability at the glenohumeral joint in humans. It is observed that in sporting activities or careers that involve frequent arm abduction, injuries to this tendon are a common cause of discomfort. Therefore, this paper evaluates the relative modelling capabilities of three hyperelastic models, namely the Yeoh, Ogden and Martins material models on the tensile behaviour of three tendon specimens. The fitting accuracies, convergence rates during optimisation, and the different forms of sensitivities to data-related features and initial parameter estimates are investigated in this study. The study finds that the Martins model outperforms the other models in fitting accuracies; the Yeoh model has the most stable performance across all initial parameter estimates (with correlations above 99 %) and has the fastest convergence rates (above 20 and 8 times as fast as the Ogden and Martins models' rates, respectively); and that the Ogden model does not depend on differences in the topological features of the test data. The material parameters of relevant constitutive models may be used for further development of computational models.

Keywords: Hyperelastic model, tendon tensile behaviour, sensitivity analysis, strain energy density function.

1. Introduction

Tendons are stiff fibrous connective tissues that facilitate the transmission of muscle forces to bones across joints [1-3]. They are parallel-fibred tissues whose dominant structural component is type I collagen. By composition, type I collagen constitutes about 60 % of the dry mass of the tendon, which is approximately 95 % of the total collagen [1, 4]. In terms of their mechanical properties, tendons are viscoelastic, and this causes them to be less effective in transmitting mechanical loads at very low strain rates, while being more effective at moving large loads at very high strain rates [1]. This is why a tendon typically exhibits increased elastic stiffness and ultimate tensile strength (UTS) with increased strain rates [2]. However, not all physical activity requires innovation of high strain rates. Even in the execution of a specific task, in order to deliver a desired quality in performance, a tendon may have to be subjected to extremely low and uncomfortable levels of strain rates.

* Corresponding Author. Tel.: +27 11 471 2079
Email Address: ngwanhm@unisa.ac.za.

The accurate prediction of mechanical behaviour of tendons is vital in the development of their different healing strategies. At the same time, their mechanical behaviour cannot be accurately predicted without availability of accurate computational models, which themselves rely on the accurate mechanical characterisation of the tendons. The above cycle of dependency, is true for most engineering systems, and more so, in all types of soft tissues, which place stringent accuracy demands in both mechanical characterisation tests and computational models. Other workers [5-8] have emphasised on the importance of accurate mechanical characterisation in developing accurate computational models for myocardial muscles to predict tissue infarction. Tensile testing has been used for the understanding of mechanical behaviour of different types of soft tissue such as sclera and heart myocardium [9-11]. The development of detailed computational models based on accurate mechanical properties have proven to increase the speed in understanding the underlying mechanisms of infection of various diseases [11, 12], which further enhance the development of effective therapies.

Tendons are naturally adapted as much thinner strands as compared with the muscles to which they are connected, consequently they experience much higher stresses than the adjoining muscles for the same muscle force. Therefore, most injuries that result from mechanical overloading or overtraining tend to involve the rupture or straining of tendons. In orthopaedics, it becomes increasingly important to understand the responses of tendons to mechanical loading in order to develop potent therapies for tendon-related injuries. Lee et al. [13] report that tendon damage is caused by mechanical loading but very little is known about its aetiology. Akintunde and Miller [14] and Cook et al. [15] further state that upon healing, tendons do not normally recover their full original functionality since the scar tissue that forms after healing has structural composition and mechanical properties that are typically different from those of the original uninjured tissue.

One of the most injury-susceptible groups of tendons is the rotator cuff shown in Figure 1. This group of tendons assists in maintaining dynamic stability at the gleno-humeral joint [16]. As depicted in the figure, this joint is dynamically unstable due to the large head of the humerus, which has to be maintained at all times in a shallow glenoid fossa. One of the most important tendons in the rotator cuff is the supraspinatus which originates from the supraspinatus muscle and inserts on to the head of the humerus. In its function to keep the humerus head in the glenoid fossa, the supraspinatus undergoes substantial tension, among two other important forms of loading, namely abrasion and lateral compression. Lewis [16] reports that injuries to the shoulder soft tissues are a principal cause of discomfort, and that this is common in people with careers that involve a lot of arm abduction such as painting, or in sports such as cricket, tennis or baseball. Several researchers [17-20] report various contradictory findings on the basic science mechanisms governing tendon injury, healing, treatment and rehabilitation. However, in order to understand the underlying mechanisms of tendon injury, it is necessary to have accurate models for its mechanical behaviour under loading.

The supraspinatus is highly stressed and experiences different types of loading in its physiological function. In its everyday operation, the supraspinatus is subjected to every type of imaginable loading from abrasion and lateral compression between the acromion process and the scapula, to the tension along its longitudinal axis. The effects of abrasion and lateral compression are somehow alleviated by the bursa that is located between itself and the acromion process. Therefore, this study focuses on modelling the mechanical response of tendons during uniaxial tensile loading which results from excessive arm abduction and adduction processes.

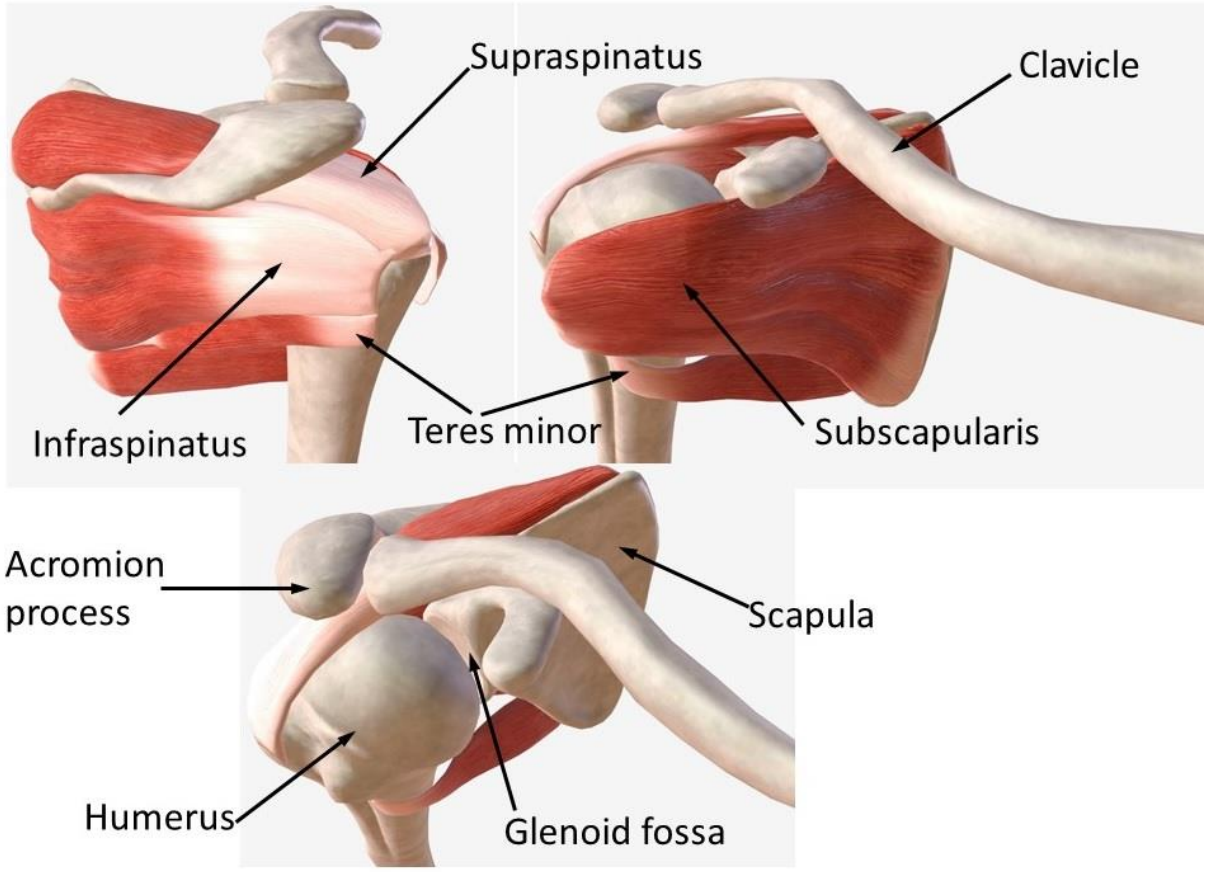

Figure 1. The anatomy of the right shoulder joint only displaying the important bones and the rotator cuff muscles and tendons.

In this paper, the computational performances of three hyperelastic models, namely, the Yeoh, Ogden, and Martins material models are evaluated. The selection of only these three material models is motivated by the findings of Martins et al. [21] where it was reported that they outperformed four other material models in terms of their approximations of tensile stress-strain behaviour in silicone-rubber and pig soft tissue. It was further observed that these three models generally yielded better fitting accuracies on silicone rubber than on the soft tissue test results. This paper explores the performances of these three models and further investigate their sensitivities to changes in test data start points, endpoints and initial parameter estimates.

2. Theoretical background

All the three models studied in this paper are hyperelastic in nature, which typically represents the mechanical behaviour of materials based on the derivation of their strain energy density function. This theory was originally formulated for hyperelastic materials of elastomeric nature, such as silicone-rubber. Therefore, in its application to this modelling approach, the subtle similarities between three specimens extracted from the supraspinatus tendon are exploited. However, this approach has its limitations which are properly reflected by the accuracy of the obtained results reported later. In hyperelasticity, material behaviour is modelled using a strain energy density function expressed by $\psi = \psi(I_i)$ which depends symmetrically on the strain invariants (I_i), which are themselves functions of the principal stretches (λ_i), where the index $i = \{1,2,3\}$ represents the three principal axes in the Cartesian

coordinate system. For incompressible materials subjected to uni-axial tension or compression, Rivlin [22] expresses the Cauchy stress σ as

$$\sigma = 2\left(\lambda_1^2 - \frac{1}{\lambda_1}\right)\left(\frac{\partial \psi}{\partial I_1} + \frac{\partial \psi}{\partial I_2}\right) \tag{1}$$

where the principal stretch λ is only considered in the axial direction $i=1$, the strain energy function ψ is only differentiated with respect to two strain invariants $\{I_1, I_2\}$ due to incompressibility considerations, and takes different forms according to the selected hyperelastic constitutive model. The strain energy functions and the respective Cauchy stresses for the three material models studied in this paper are presented below [21,23,24].

For the Yeoh material model, the strain energy function is given by [23]

$$\psi_Y = \sum_{j=1}^{3} c_j \left(I_1 - 3\right)^j \tag{2}$$

where c denotes material parameters and the indices $j = \{1,2,3\}$ represent the three different parameter values. Thus the Cauchy stress is calculated from Eqs. (1) and (2) and expressed as [23]

$$\sigma_Y = 2\left(\lambda_1^2 - \frac{1}{\lambda_1}\right)\left(c_1 + 2c_2\left(I_1 - 3\right) + 3c_3\left(I_1 - 3\right)^2\right) \tag{3}$$

For the Ogden material model, the strain energy function is given by [24]

$$\psi_O = \sum_{i=1}^{3} \frac{c_{(2i-1)}}{c_{2i}}\left(\lambda_1^{c_{2i}} + \lambda_2^{c_{2i}} + \lambda_3^{c_{2i}} - 3\right) \tag{4}$$

Upon applying the mathematical operation in Eq (1), the Cauchy stress for the Ogden material model for uni-axial extension can be written as [24]

$$\sigma_O = c_1\left[\lambda_1^{(c_2-1)} - \lambda_1^{\left(-\frac{c_2}{2}-1\right)}\right] + c_3\left[\lambda_1^{(c_4-1)} - \lambda_1^{\left(-\frac{c_4}{2}-1\right)}\right] + c_5\left[\lambda_1^{(c_6-1)} - \lambda_1^{\left(-\frac{c_6}{2}-1\right)}\right] \tag{5}$$

For Martins material model, the strain energy function is given by [21],

$$\psi_M = c_1\left(e^{c_2(I_1-3)} - 1\right) + c_3\left(e^{c_4(\lambda-1)^i} - 1\right) \tag{6}$$

The Cauchy stress for the Martins material model can therefore be determined as [21]

$$\sigma_M = 2\left(\lambda_1^2 - \frac{1}{\lambda_1}\right)c_1c_2e^{c_2(I_1-3)} + 2\lambda_1\left(\lambda_1 - 1\right)c_3c_4e^{c_3(\lambda_1-1)^2} \tag{7}$$

In each of these models, the material parameters c are nonlinear elastic parameters and are implicit functions of the measured stresses. It is only for a neo-Hookean model where these parameters can be directly related to the measured stresses. In order to determine the Cauchy stresses, we solve for the parameters whose values minimise the squared-error

between the measured stresses σ_{exp} and model predicted stresses σ_{mod}. Thus for all the three material models in Eqs (3,5,7), the optimization problem can be expressed as:

$$\min_{c} \sum \left(\sigma_{\text{mod}} - \sigma_{\text{exp}} \right)^2 \tag{8}$$

where σ_{mod} is the Cauchy stress for a particular material model as given in Eqs (3,5,7). The squared error are optimised with respect to material parameters, c. For all the three models, the parameters were solved using a nonlinear least squares curve fitting routine in MATLAB, employing a default 'trust-region-reflective' algorithm. This algorithm is a subspace trust region algorithm for large-scale problems, which is based on the interior-reflective Newton method (Mathworks® Inc., [25]). Each iteration involves the approximate solution of a large linear system using the method of preconditioned conjugate gradients. However, this algorithm does not accept underdetermined systems, so in those cases, the Levenberg-Marquardt algorithm might be recommended. The present algorithm can be used in small-to-medium scale problems without computing the Jacobian or providing the Jacobian sparsity pattern, which makes the process much faster than the routines that compute the Jacobian.

3. Materials and Methods

Prior to testing, the specimens were stored in situ (within the shoulder joint) in a frozen state (typically below zero degree Celcius). Normal sterilised surgical knives and stainless steel tweezers were used to excise the specimens from the host cadaver shoulders after which the specimens were temporarily (less than 5 min) wrapped in a saline-moistened gauze [2] before clamping them in the testing machine to avoid over-hydration. Before excision, the shoulders were allowed to defrost under room temperatures between 34^{o}C and 37 ^{o}C. The testing was conducted under these room temperatures having relative humidity between 60 % and 100 %. The harvested specimens were of different average cross sectional areas: 90 mm^2, 70 mm^2 and 50 mm^2 with lengths of 50±2 mm. The tendon ends were clamped between two parallel plates whose gripping surfaces were tightly bonded with grade P60 sandpaper to reduce slippage of the tendon between the plates during testing. Although some amount of slippage might have occurred within the inner layers of the tendon tissue, it is expected that such slippage was insignificant within the linear elastic phase before the failure stages of the tendon tissue, and therefore might have negligible effect within the test region of study in this paper. Owing to the scarcity of these test specimens, no risks were taken to precondition them before the actual testing.

The MTS EM Tensile tester was operated in displacement control at an average strain rate of 1.72 % s^{-1} for all the three tests as shown in Figure 2. As shown in the figure, it was extremely hard to maintain a constant strain rate and Test 3 shows a particularly high deviation in the strain rates. The tests were not conducted in any environmental chamber and all the tests were performed under room air temperature conditions up to rupture. The data were recorded through a MTS TestSuite on a dedicated computer and recorded in separate excel data sheets which were later exported to MATLAB for post processing.

The Yeoh, Ogden and Martins material models were programmed in MATLAB and later modelled in Simulink (see the Simulink models in the Appendix) for the sensitivity analysis. The purpose of the sensitivity analysis was to refine the fitting accuracy by focussing the optimisation procedure on the more sensitive material parameters. In order to implement the sensitivity analysis, the material models were developed in MATLAB/Simulink in which the

material parameters were used as design variables. The optimal values as obtained from the initial optimisation process were used to prescribe the search ranges. Thirty data points were generated within each search range using the Latin hypercube method in MATLAB. This method typically generates parameter samples that systematically fills up the given space or range. Correlation plots of the material parameters were plotted in a scatter plot to detect the existence of any underlying correlations between the different material parameters. In case of any direct correlations, it would be appropriate to ignore one of the correlated material parameters to reduce the computational overhead during the sensitivity analysis. All the parameters in all the three material models showed no correlations as shown in Figure 3. Therefore the sensitivity exploration was conducted on all the parameters for all the three material models.

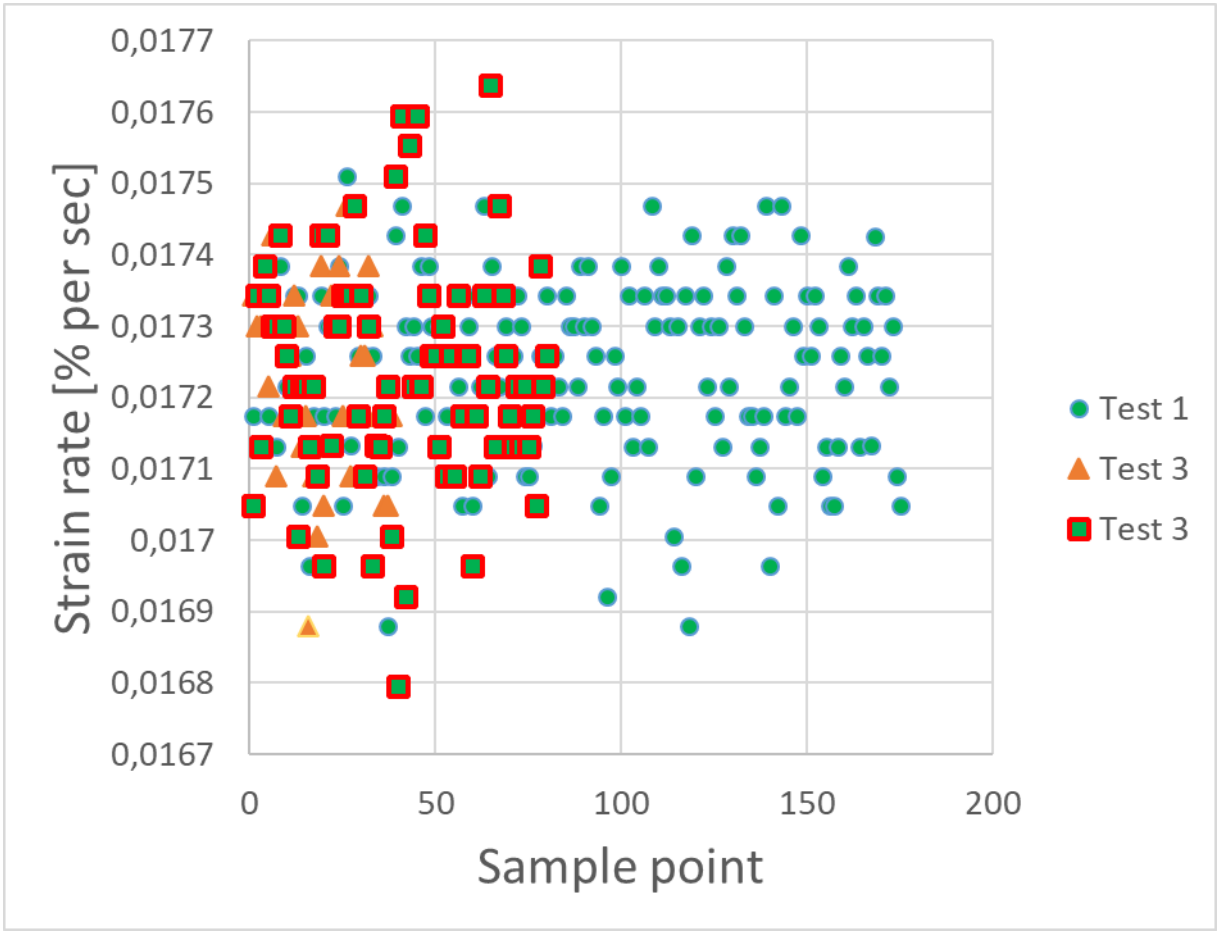

Figure 2. A cluster plot of strain rates for each test.

The sensitivities for each of the material parameters were calculated. The material parameters which yielded sensitivities higher than 0.5 were considered to exert significant influence on the square-error between model-calculated stress and measured stress. Thereafter, the optimisation was run for those parameters with high enough sensitivities while keeping the rest of the parameters constant at their initial values. The final optimal values are the ones that were used to determine the Cauchy stresses.

Upon further analysis of the results, it was observed that the performance of the material models changed with different start- and end-points in the measured data range. As a result, this behaviour was investigated in the three tests through three-dimensional surface plots of correlation percentages of the three material models for various combinations of start points and end points in the form of surface plots. The data were linearly interpolated for a total of

512 sample points to allow for better investigation of this behaviour. In the plotted surface plots, the point number from which the data range started was denoted as “Delay”, while the number of samples which were cut out from the end-points of the original data range is called the “Upper cut-off”. The ranges of Delay were arbitrarily prescribed from 0 to 30 data points in steps of one data point, while the Upper cut-off ranges were prescribed from 0 to 150 data points in steps of 5 data points. This implies that a particular combination with Delay = 0 and Upper cut-off = 0 would mean that the original full data range was maintained, while that with Delay = N_d and Upper cut-off = N_u would mean that its data range is from the sample point number (N_d+1) up to a sample point number (N-N_u). In total, there were 961 different combinations of data sets investigated for each test and each model. Thus there are combinations of error points which were calculated for material models per test.

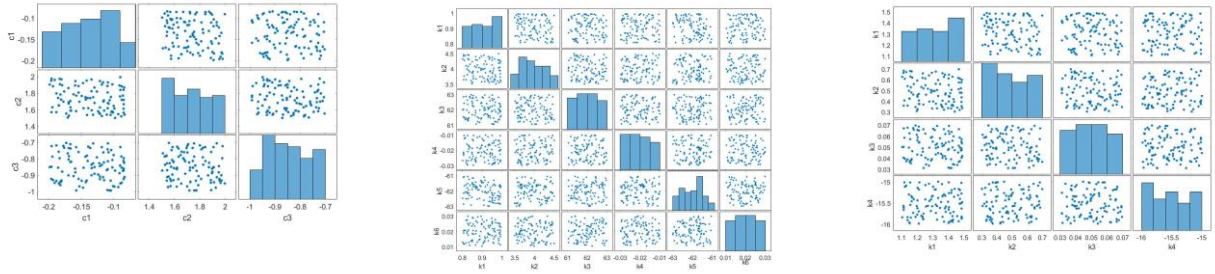

(a) (b) (c)

Figure 3. Scatter plots of the generated parameter sample space showing parameter correlations in (a) Yeoh (b) Ogden (c) Martins material models.

In addition to the above investigation, the influence of initial parameter estimates were explored. Eleven different initial seeds in the range {-10, 10} were applied to the models for each test. These results were examined through line graphs showing fitting errors and correlation percentages for each model and test.

4. Results and Discussions

The reported results are only for the combinations of start points and endpoints that yielded maximum correlations with experimental data for each model. This is why there are some differences in the start points and endpoints of the results. For example, the Martins model shows that the combinations that yielded its maximum correlation had a much larger start point and endpoint in test 1 than the Yeoh and Ogden models which had similar start points and endpoints. For test 2, only the Martins model had a much longer start delay but the endpoint is similar to the other models. In test 3, all models have similar start points and endpoint. For all the reported results, initial parameter estimates were set at a value of 5. The choice of this initial parameter estimate was based on the fact that all the models had their best performances within an initial parameter estimate range of {2, 8}. The results in Figures 4-6 show levels of correlations in the frames labelled as (a), and fitting errors in the frames labelled as (b) for all three tests. The results show that the Martins model slightly outperforms the other two models with minimum level of correlation at 99.8 % and a fitting error of less than 5 %. This is largely attributable to its model formulation which is dependent on the principal stretches, the first principal strain, and the fibre direction which are not applicable for either the Yeoh or Ogden models. It is observed that this performance is not influenced by the number of the material parameters, since the Ogden material model which has the largest number of material parameters does not perform very well. The Yeoh model has three

material parameters and depends on the principal stretch and the first principal strain only, while the Ogden model depends solely on the principal stretch.

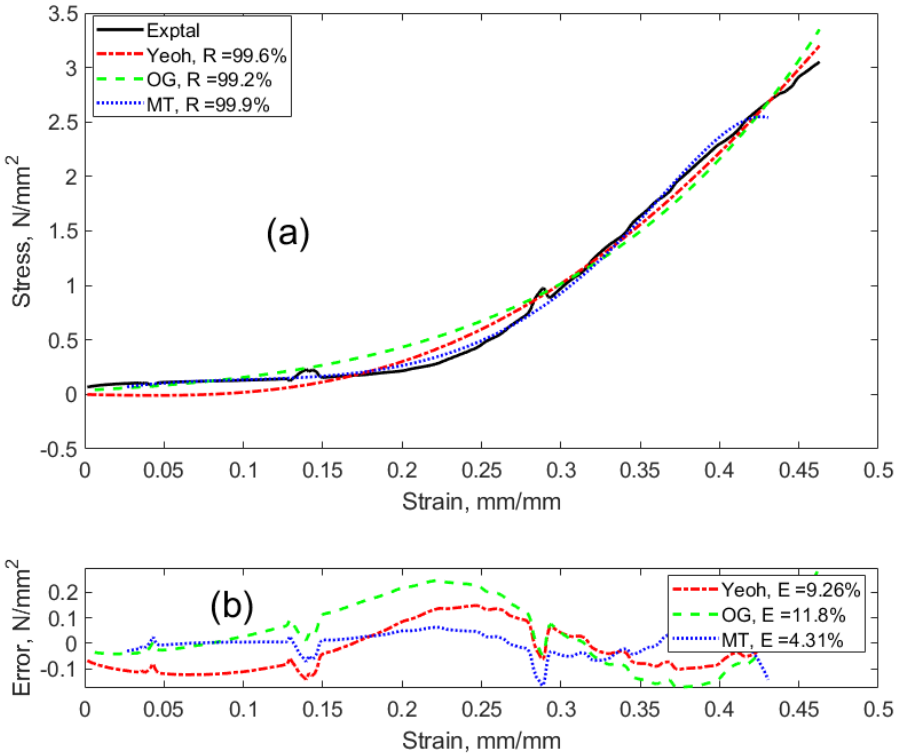

Figure 4. Model results correlated with test 1 data and corresponding fitting errors.

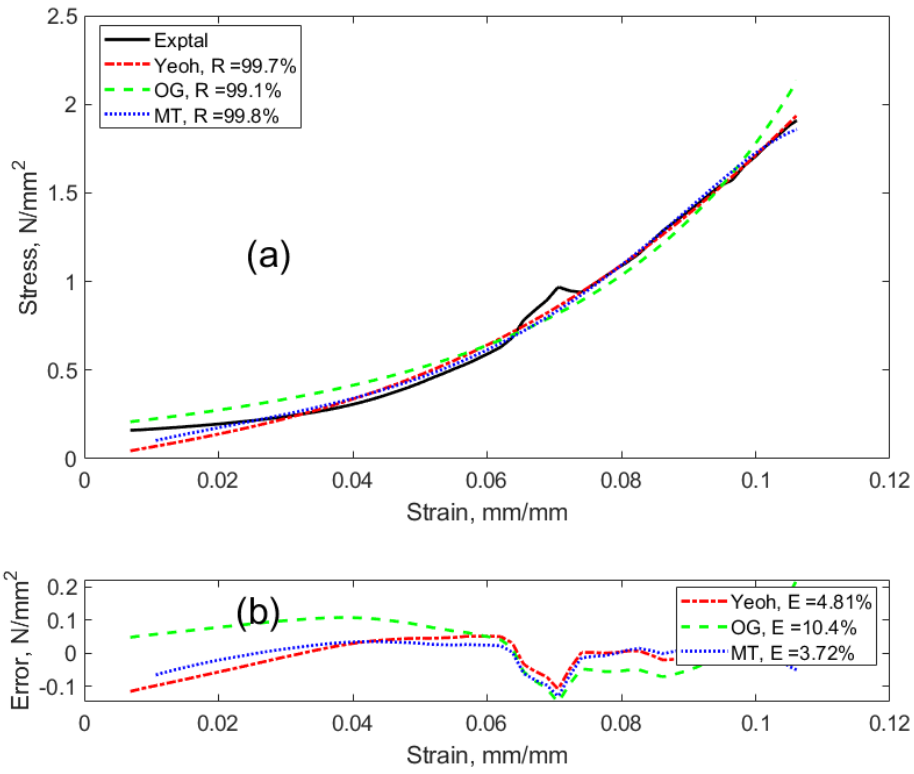

Figure 5. Model results correlated with test 2 data and corresponding fitting errors.

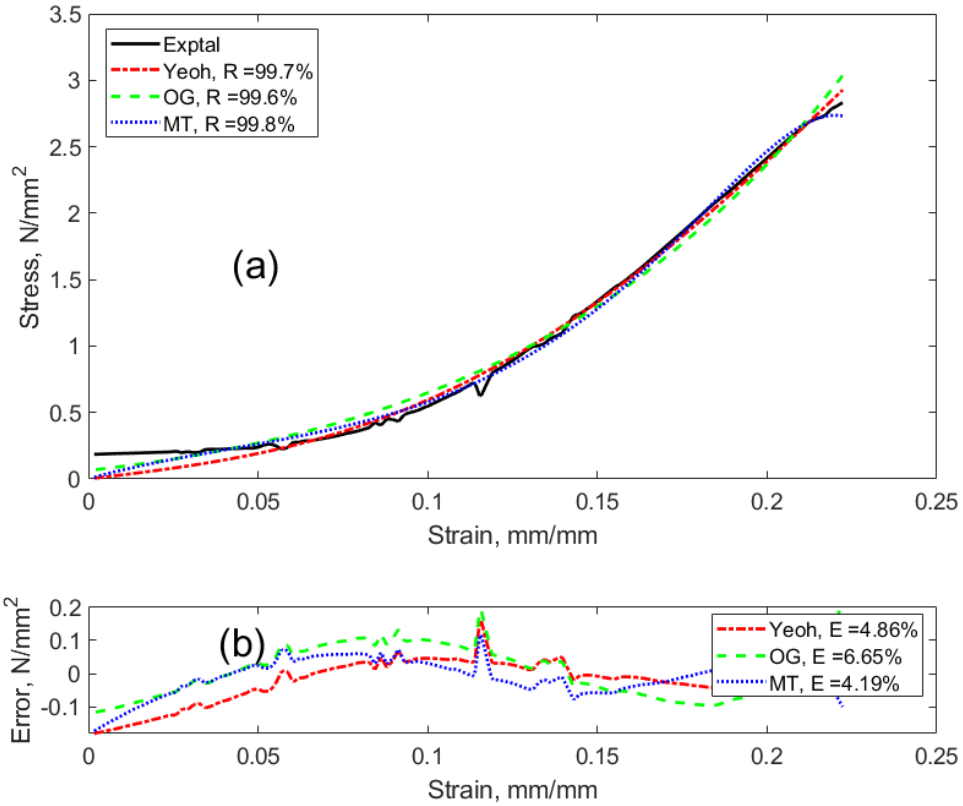

Figure 6. Model results correlated with test 3 data and corresponding fitting errors.

Typically, all the three models perform poorly in the toe regions as compared to the linear elastic regions. Yeoh [23] shows that such errors in regions of small strains are due to the inability of the shear modulus to perfectly follow the soft tissue shear modulus. Martins et al. [21] further elaborate on this by stating that such errors are caused by the non-homogeneity and compressibility effects of soft tissues which are not sufficiently modelled by strain energy density functions. In addition to this, there are also marked deviations at the transitions between the toe region and linear region in all the test data, which cannot be modelled by any of the three models. Because it is not clear what causes such discontinuity, further investigation might be justifiable since this occurs in all the three tests.

Table 1 shows the material parameters and convergence rate results of the optimisation processes for the three models on each test. The Yeoh model converges much faster than both the Ogden and Martins models. The results show that it converges over 20, and 8 times as fast as the Ogden and Martins models, respectively. This is largely due to its reduced number of function evaluations and number of required parameters as shown in Table 1. This gives it a big advantage over the Martins model when compared to the minor differences between the two models in correlations and fitting accuracies.

Table 1 shows that the optimisation processes on test 2 are the most computationally challenging on the Yeoh and Martins models. This is evident from the much wider spreads in the values of the optimal material parameters and from the higher numbers of iterations as compared to the other two tests. An examination of the original measured data reveals that test 2 has a shorter toe region followed by a much steeper linear region as compared to the other tests. Between test 1 and 3, it is test 3 that has a shorter toe region and steeper linear region. This is also reflected in the relatively higher iteration numbers for test 3 when compared with test 1 for the Yeoh and Martins models. Therefore it would seem that the

length of the optimisation processes in the Yeoh and Martins models rely on the topological features of the test data both in the toe and linear region. On the other hand, the Ogden model is insensitive to these topological features as far as length of optimisation processes are concerned. The Ogden model only reflects these relative difficulties with optimisation processes through the amount of spread in the values of the optimal material parameters as shown in Table 1.

Table 1. Material parameters for each model over each test.

Model		**Test 1**	**Test 2**	**Test 3**
Yeoh	Material parameters	-0.0498 1.4693 -0.4438	1.0772 35.2127 -90.4680	0.5100 9.0520 -13.7950
	Iterations	2	4	2
	Function evaluations	12	20	12
Ogden	Material parameters	-0.0572 2.6988 0.3693 9.6320 -0.2782 9.6444	0.0012 59.3954 -1.0973 -1.1385 0.0678 29.5417	-0.0007 3.9542 -0.3142 4.2327 0.3698 11.5638
	Iterations	85	85	85
	Function evaluations	602	602	602
Martins	Material parameters	4.5734 1.4996 9.6464 -1.9512	46.8614 0.8189 125.9407 -0.8685	13.6473 1.0691 33.5004 -1.1958
	Iterations	16	59	22
	Function evaluations	85	300	115

Test results show that there are differences in the definitions of the toe regions, the steepness of the linear regions, and magnitudes of stress and strains at the points close to the UTS. Viidik [2] found that these differences are caused by a specimen's strain history, water content, specimen geometry and strain rates. During specimen dissection or excision, care should be taken to either avoid prestraining the specimens or to ensure consistency in the process of specimen dissection. In terms of water content, it was pointed out that overhydration lowers the elastic stiffness. It was also shown that shorter (< 10 mm long) soft tissue specimen exhibited a wide sensitivity range in their mechanical properties. Viidik [2] further showed that higher strain rates increased both elastic stiffness and UTS magnitudes, while Wren et al. [26] agreed with the increase in UTS magnitudes but argued that the elastic stiffness remained unchanged. In this study, the strain rates were kept reasonably constant on

all tests, and all the three specimens were equally wrapped in saline gauze for similar lengths of duration. Therefore differences in strain histories and specimen geometry, (evident from the differences in the ratios between cross-sectional areas to specimen lengths) may have played a major role in the observed differences in this study. We further hypothesize that differences in the prevailing laboratory temperatures from one test to another may have slightly affected the test results.

Figure 7 shows surface plots of correlations on all three tests. The detailed descriptions of "Delay" and "Upper cut-off" are presented in Section 3. It is shown that only the Yeoh model exhibits smoother surfaces (> 99 %) without significant deviations, while the other models (especially the Ogden model) have high levels of deviations in the surface plots (above 90 %). This implies that despite the reported best performance of the Martins model in the fitting accuracy results, the Yeoh model is more stable at any given data range. On all tests, the Yeoh model shows that correlations are highest along the zero start point line. It further shows that correlations are more sensitive to start point changes than endpoint changes. With the exception of test 2, the Ogden model displays rather random behaviour, it shows a decrease in the correlations at longer start points. This might be a reflection of the non-convexity and non-uniqueness problems in the Ogden model as reported by some authors [27,28]. Although test 2 is largely smooth, it still has two outliers located on the negative correlation side.

The result of the Martins model along lines very close to zero start points is rather surprising since it cannot be observed in the other tests. Test 1 is shown to be uncharacteristically elongated in its toe region although its impact seems to have more effect on the Martins model. Therefore, the Martins model does not yield the highest correlations along the zero start point line for test 1.

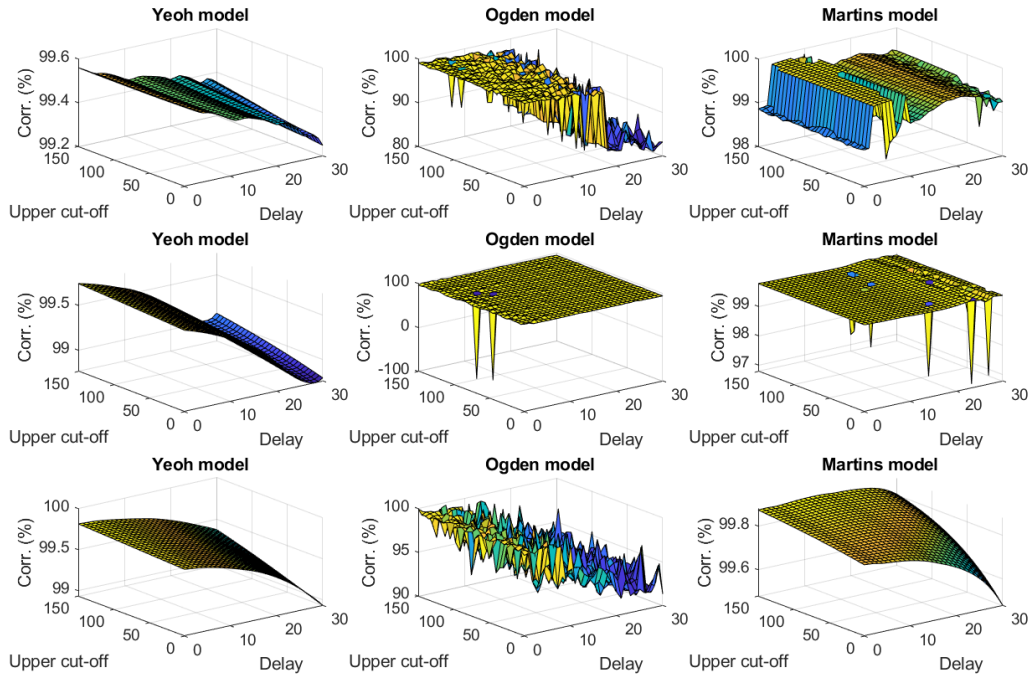

Figure 7. Surface plots of model results correlations (%) with test results for all three tests.

Figures 8 and 9 show that all the three models perform the best when the initial parameter values lie in the range between 2 and 8. The Ogden model is extremely poor on the negative

side of the initial parameter estimates almost for all tests and the Martins model is very poor at an initial parameter estimate of zero. Only the Yeoh model shows stable performance over the entire range of the initial parameter estimates. Its correlations remain above 99 % with fitting errors of less than 10 % for all seeding conditions.

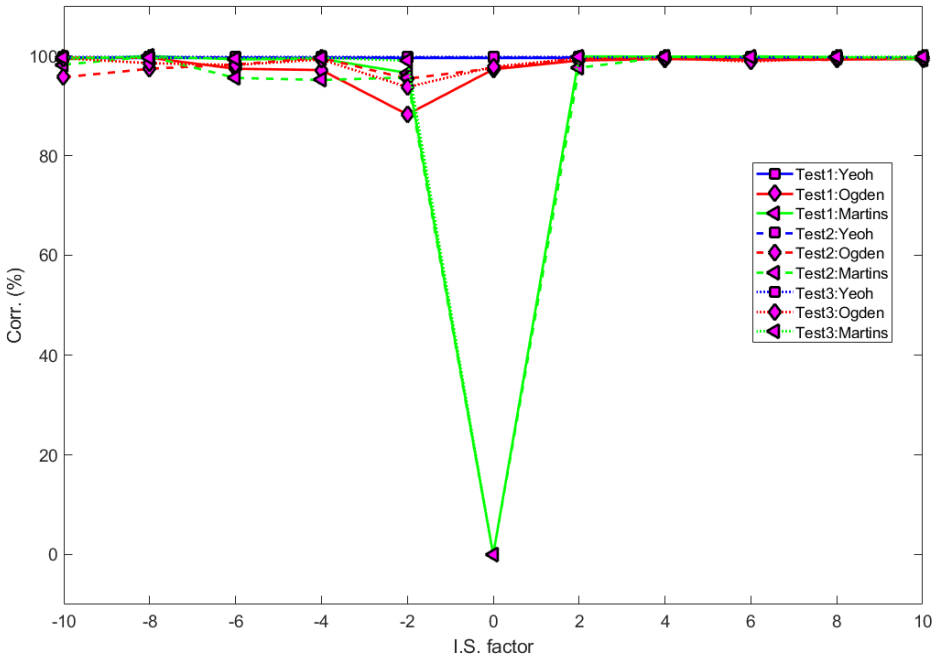

Figure 8. Comparison of correlations (%) variation due to different values of initial seeding (I.S.).

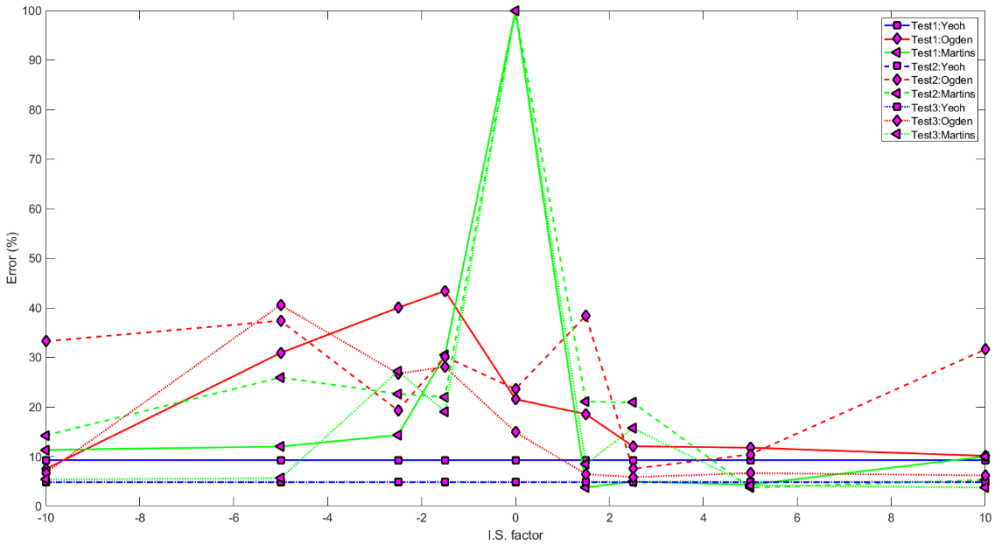

Figure 9. Influence of initial seeding (I.S.) on the fitting errors (%).

A sensitivity analysis of the parameters for each model around their optimal values as obtained from the nonlinear least squares technique was performed for further refinement of

the results. The analysis was performed using Simulink models in which each of the parameters for each model were selected as design variables, and the cost function was the error between the test and model calculated stresses. Thirty sample points were generated for each design variable and their scatter plots showed that they were actually uncorrelated with each other. This gave us confidence that the chosen design variables were actually unrelated to each other (no redundancy). Later, a sensitivity study showed that the Yeoh model yielded higher sensitivity above 0.7 only for parameter c_2, while those yielded for parameters c_1 and c_3 were less than 0.3. Therefore, only c_2 was optimised further while c_1 and c_3 were held at their original values. The new parameters were used to recalculate the Yeoh stresses, but there was no significant improvement in the calculated Cauchy stresses. The Ogden and Martins models yielded sensitivities below 0.3. As a result, it was concluded that the calculated stresses for these models are quite insensitive to parameter changes around their optimal parameter values as obtained by the nonlinear least squares method used in this technique. It can be further concluded that the nonlinear least squares optimisation technique is quite satisfactory in determining the optimal parameter values without any need for further refinement of the optimal values for all three models.

5. Conclusion

This paper evaluates the computational performances of three hyperelastic material models, namely the Yeoh, Ogden and Martins models. Although all the models are derived from the strain energy density function, they are actually dependent on different factors. The Yeoh model is dependent on the principal stretch and the first strain invariant; the Ogden model is only dependent on the principal stretch; and the Martins model is dependent on the principal stretch, first strain invariant and the fibre direction. The fitting performances of these models on tendon tissue tensile behaviour seem to be influenced by these factors, as it is found that the Martins model yields the highest fitting accuracies with correlations of above 99.8 % and fitting errors of less than 5 %. The Yeoh model is second with correlations of above 99.6 % and fitting errors of less than 10 %; while the Ogden model has a minimum correlation of 99.1 % with fitting errors under 12 %. So, modelling of fibre direction in soft tissue is an important factor if accurate fitting accuracies have to be obtained. However, it should be emphasised that these results were evaluated from combinations of start and endpoints that yielded maximum correlations for each model. Therefore, post-processing should involve the identification of test data ranges that can produce such high correlations if these results are to be reproduced in any given test data. This is the case especially for the Martins and Ogden models, which show high deviations to changes in test data ranges.

When comparing the optimisation efficiencies, it was found that the Yeoh model had the fastest convergence rates on all the three tests. Its convergence speed is 8 times as fast as that of the Martins model and 20 times as fast as that of the Ogden model. This speed advantage may offset any benefits obtained from the better fitting accuracies of the Martins model. Furthermore, in terms of its sensitivity to initial parameter estimate changes, the Yeoh model is also the most stable. The Martins model yields very poor results at initial parameter estimates around zero, while the Ogden model does not perform very well with negative initial parameter estimates for all the tests reported in this paper.

The Ogden model shows that it is insensitive to test data topological features. While the Yeoh and Martins models change from 2 to 4 iterations and from 16 to 59 iterations respectively, from test 1 to test 2 due to the differences in these features. The Ogden model remains at 85 iterations for both tests with the only notable changes occurring in the spread of the optimal parameters between the two tests.

However, all the three models yield relatively lower fitting accuracies in the toe regions than in the linear regions on all tests. These findings are in support of those found in Martins et al. [21]. Mooney [29] hypothesises that strain energy function-based hyperelastic models are incapable of accurately modelling mechanical behaviour in small strains even when the theory is extended to the second or higher orders of approximation.

In conclusion, it is shown that each of the three models have their strengths and weaknesses, although it is generally observed in this study that the Yeoh model has more significant benefits owing to its relatively excellent convergence rates during optimisation, its stability across different test data ranges and its good fitting accuracies. We further observe that modelling of fibre direction, especially in soft tissue, effects some improvements in the fitting accuracies. For further study, we recommend more investigation into tissue modelling in the regions of small strains where these models yield relatively poorer correlations. Directly linked to this is the need for the development of better testing techniques, facilities and specimen preparation procedures to ensure test result reproduction in regions of small strains, as this may assist in understanding complex tissue behaviour under physiological conditions.

6. Acknowledgements

We would like to acknowledge Tsitsi Makina of the University of South Africa for language editing services.

7. Author Contributions

H.M. Ngwangwa and F. Nemavhola contributed equally towards the conception and design of the research project, the analysis and interpretation of the data, and the writing of the paper. Both authors have critically reviewed its contents and have approved the final version submitted for publication.

References

[1] J.H-C. Wang, Mechanobiology of tendon, *Journal of Biomechanics,* Vol. 39, No. 9, pp.1563-1582, 2006.

[2] A. Viidik, 1987, Biomechanics of tendons and other soft connective tissues. Testing methods and structure-function interdependence, in *Biomechanics: Basic and Applied Research* edited by G. Bergmann, R. Köbel, A. Rohlmann, Kluwer Academic Publishers, Dordrecht.

[3] J.G. Snedeker, J. Foolen, Tendon injury and repair – A perspective on the basic mechanisms of tendon disease and future clinical therapy, *Acta Biomaterialia,* Vol. 63, pp. 18-36, 2017.

[4] Y.C. Fung, 1993, *Biomechanics: Mechanical properties of living tissues,* Springer, New York.

[5] F.J. Masithulela, 2016, Computational biomechanics in the remodelling rat heart post myocardial infarction, PhD Thesis, University of Cape Town.

[6] F. Masithulela, Bi-ventricular finite element model of right ventricle overload in the healthy rat heart, *Bio-medical Materials Engineering*, Vol. 27, No. 5, pp. 507-525, 2006.

[7] F. Nemavhola, Detailed structural assessment of healthy interventricular septum in the presence of remodelling infarct in the free wall – A finite element model, *Heliyon*, Vol. 5, No. 6, e01841, 2019.

[8] F. Nemavhola, Fibrotic infarction on the LV free wall may alter the mechanics of healthy septal wall during passive filling, *Bio-medical Materials Engineering*, Vol. 28, No. 6, pp. 579-599, 2017.

[9] Z. Ndlovu, F. Nemavhola, D. Desai, Biaxial mechanical characterization and constitutive modelling of sheep sclera soft tissue, *Russian Journal of Biomechanics*, Vol. 24, No. 1, pp. 84-96 , 2020.

[10] F. Nemavhola, Biaxial quantification of passive porcine myocardium elastic properties by region, *Engineering Solid Mechanics*, Vol. 5, No. 3, 155-166, 2017.

[11] F. Masithulela, The effect of over-loaded right ventricle during passive filling in rat filling heart: A biventricular finite element model, *ASME International Mechanical Engineering Congress and Exposition*, Vol. 3, 57380, V003T03A005, 2015.

[12] F. Masithulela, Analysis of passive filling with fibrotic myocardium infarction, *ASME International Mechanical Engineering Congress and Exposition*, Vol. 3, 57380, V003T03A004, 2015.

[13] A.H. Lee, S.E. Szczesny, M.H. Santare, D.M. Elliott, Investigating mechanisms of tendon damage by measuring multi-scale recovery following tensile loading, *Acta Biomaterialia*, Vol. 57, pp. 363-372, 2017.

[14] A.R. Akintunde, K.S. Miller, Evaluation of microstructurally motivated constitutive models to describe age-dependent tendon healing, *Biomechanics and Modeling in Mechanobiology*, Vol. 17, pp. 793-814, 2018.

[15] J.L. Cook, E. Rio, C.R. Purdam, S.I. Docking, Revisiting the continuum model of tendon pathology: what is its merit in clinical practice and research? *British Journal Sports Medicine*, Vol. 50, No. 19, pp. 1187-1191, 2016.

[16] J.S. Lewis, Rotator cuff tendinopathy: a model for the continuum of pathology and related management, *British Journal Sports Medicine*, Vol 44, No. 13, pp. 918-923, 2010.

[17] B.R. Freedman, J.A. Gordon, L.J. Soslowsky, The Achilles tendon: fundamanetal properties and mechanisms governing healing, *Muscles Ligaments Tendons Journal*, Vol. 4, No. 2, pp. 245-255, 2014.

[18] N.L. Leong, J.L. Kator, T.L. Clemens, A. James, M. Enamoto-Iwamoto, J. Jiang, Tendon and ligament healing and current approaches to tendon and ligament regeneration, *Journal of Orthopaedic Research*, Vol. 38, No. 1, pp. 7-12, 2020.

[19] S.E. Szczesny, D.M. Elliot, Incorporating plasticity of the interfibrillar matrix in shear lag models is necessary to replicate the multiscale mechanics of tendon fascicles, *Journal of the Mechanical Behaviour of Biomedical Materials*, Vol. 40, pp. 325-338, 2014.

[20] B.N. Safa, A.H. Lee, M.H. Santare, D.M. Elliott, Evaluating plastic deformation and damage as potential mechanisms for tendon inelasticity using a reactive modeling

framework, *Journal of Biomechanical Engineering*, Vol. 141, No. 10, 1010081-10100810, 2019.

[21] P.A.L.S. Martins, R.M. Natal Jorge, A.J.M. Ferreira, A comparative study of several material models for prediction of hyperelastic properties: application to silicone-rubber and soft tissues, *Strain*, Vol. 42, No. 3, 135-147, 2006.

[22] R.S. Rivlin, Large elastic deformations of isotropic materials. IV. Further developments of the general theory, *Philosophical Transactions of the Royal Society of London A*, Vol. 241, No. 835, pp. 379-397, 1948.

[23] O.H. Yeoh, Some forms of the strain energy function for rubber, *Rubber Chemistry and Technology*, Vol. 66, No. 5, pp. 754-771, 1993.

[24] R.W. Ogden, 1984, *Non-linear elastic deformations*, Dover Publications, New York.

[25] Mathworks® Inc. *MATLAB, Documentation: Least-squares (model fitting) algorithms*. Accessed from https://www.mathworks.com/help/optim/ug/least-squares-model-fitting-algorithms.html on 30/12/2019.

[26] T. Wren, S. Yerby, G.S. Beaupré, D.R. Carter, Mechanical properties of the human Achilles tendon, *Clinical Biomechanics*, Vol. 16, No. 3, pp. 245-251, 2001.

[27] G.A. Holzapfel, T.C. Gasser, R.W. Ogden, A new constitutive framework for arterial wall mechanics and a comparative study of material models, *Journal of Elasticity and the Physical Science of Solids*, Vol. 61, pp. 1-48, 2000.

[28] R.W. Ogden, G. Saccomandi, I. Sgura, Fitting hyperelastic models to experimental data, *Computational Mechanics*, Vol. 34, pp. 484-502, 2004.

[29] M. Mooney, A theory of large elastic deformation, *Journal of Applied Physics*, Vol. 11, No. 9, pp. 582-592, 1940.

Appendix

In the Figures A1-A3, showing Simulink modelled material models, the material parameters are set up as gain block variables with predefined ranges around the initially calculated optimal values from the nonlinear least squares routine.

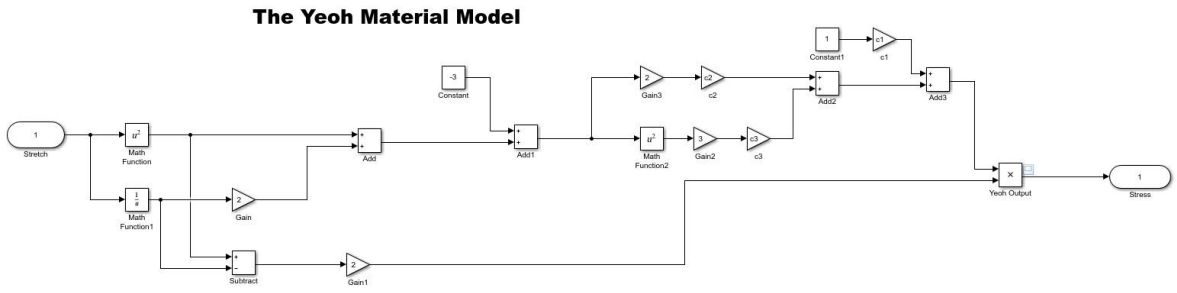

Figure A1. A Simulink Yeoh material model.

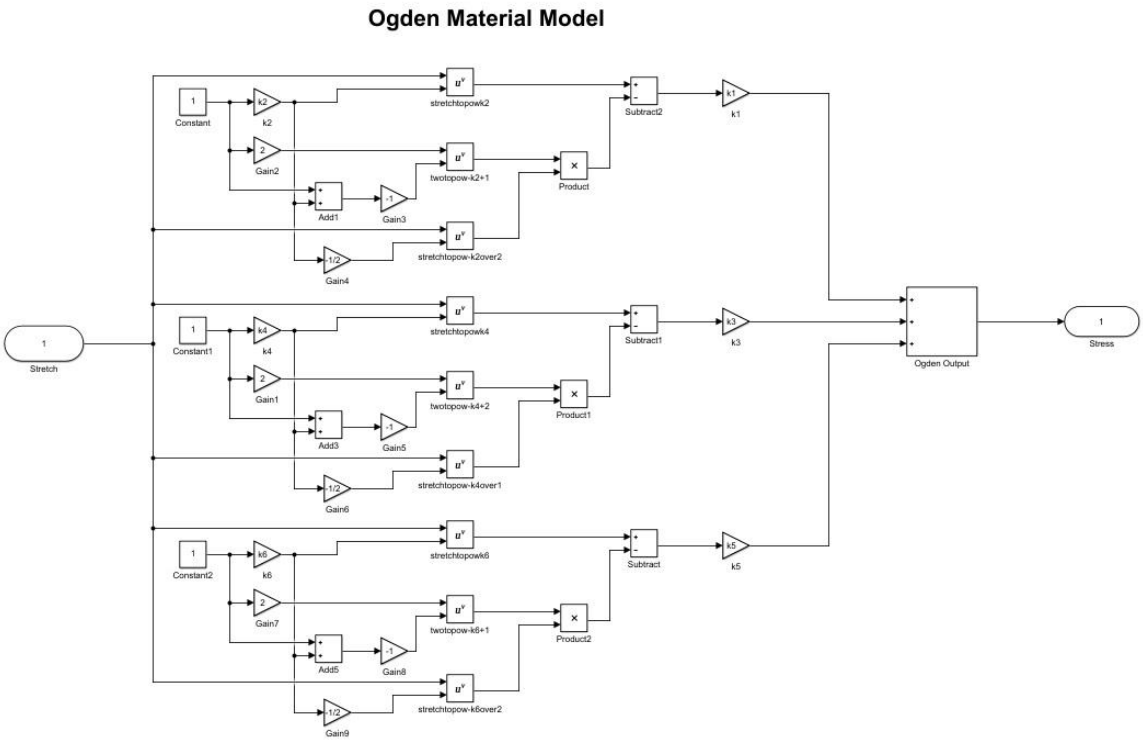

Figure A2. A Simulink Ogden material model.

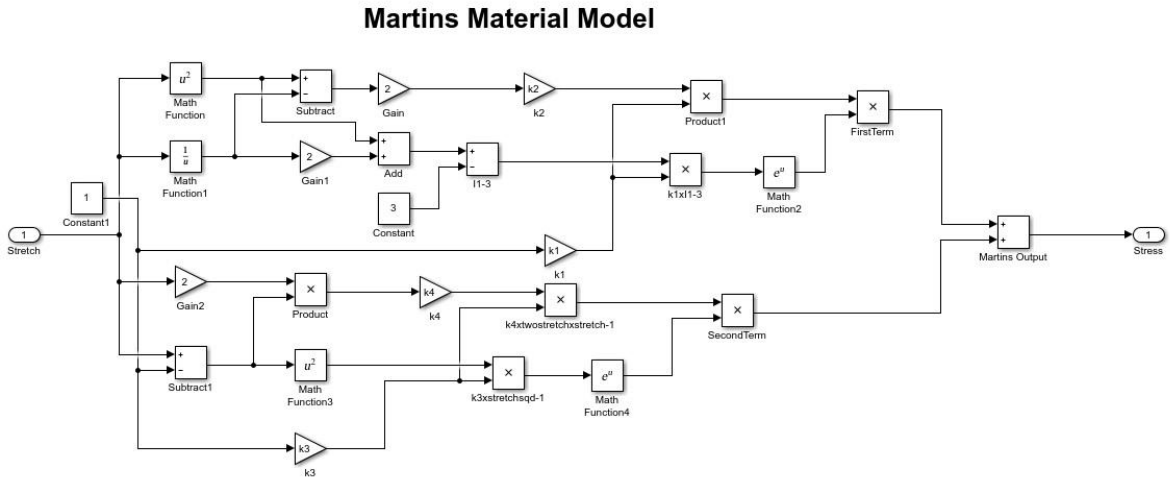

Figure A3. A Simulink Martins material model.